



ISSN 0975-413X
CODEN (USA): PCHHAX

Der Pharma Chemica, 2016, 8(1):128-136
(<http://derpharmachemica.com/archive.html>)

Crystal structure and docking analysis of (10S,13R,14S)-8,11-dimethyl-13-phenyl-12-oxa-1,11-diazatetracyclo[7.6.0.0^{2,7}.0^{10,14}]pentadeca-2,4,6,8-tetraene-14-carbonitrile

V. Sabari^{a*}, G. Suresh^b, R. Ganesan^b, G. Sivakumar^c and M. Bakthadoss^c

^aSchool of Basic Science, Vel Tech University, Chennai, India

^bDepartment of Physics, Vel Tech Multitech, Chennai, India

^cDepartment of Organic Chemistry, University of Madras, Chennai, India

ABSTRACT

Single crystals of indole (IND) moiety were grown by slow evaporation method at room temperature. Single crystal x-ray diffraction analysis reveals that indole crystallizes in Orthorhombic system with space group $Pca2_1$ and the calculated lattice parameters are $a = 16.288(4) \text{ \AA}$, $b = 6.1798(5) \text{ \AA}$, $c = 17.246(4) \text{ \AA}$. The structure of IND moiety is planar. The fused benzene and pyrrole rings creates the dihedral angle of $0.91(5)^\circ$. The five membered pyrrolidine ring adopts an envelope conformation. The other isoxalidine ring adopts an envelope conformation. In the crystal molecules are linked through intermolecular C6-H6A...N2 hydrogen bond. The packing was further stabilized by C9-H9...Cg(4) interaction. Using Schrodinger package, docking studies of the crystal structure of the RNA dependent RNA polymerase NS5B of Hepatitis C virus (HCV), with indole has been carried out.

INTRODUCTION

Indole is an aromatic heterocyclic organic compound consisting of a six-membered benzene ring fused to a five-membered nitrogen-containing pyrrole ring. Indoles are known for their important chemical, medicinal and physiological activities. The indole ring system is present in a number of natural products, many of which are found to possess pharmacological properties. Some of the indole alkaloids extracted from plants possess cytotoxic, antitumour and antiparasitic properties[1].

Indoles form an integral part of many natural products and possess potentially reactive sites to perform variety of chemical reactions to generate molecular diversity. Many of the indole derivatives possess anti-inflammatory[2], antibacterial [3], antitumour [4,5] and antifungal [6 - 9] activities.

Hepatitis is one of the most dreadful diseases known to mankind. This disease is characterized by inflammation of liver, swelling and permanent damage to liver tissues. A number of different agents causing hepatitis include infectious diseases, chemical poisons, drugs and alcohol. Viral hepatitis refers to six different viruses, namely hepatitis A (HAV), hepatitis B (HBV), hepatitis C (HCV), hepatitis D (HDV), hepatitis E (HEV) and hepatitis G (HGV). All hepatitis viruses can cause an acute (short term) form of liver disease.

Hepatitis C Viruses (HCV)

Viruses are the smallest known forms of life and are responsible for a wide range of diseases in human, ranging from the common cold, smallpox, AIDS, and hepatitis. Viruses use host cells (bacteria, plant cells, or human body cells) to reproduce themselves. Viruses insert their genetic material into the cell and transform it into a "factory" for virus production. Sooner or later this kills the infected cell causing disease. Viruses usually infect specific types of cells like human lung cells (pneumonia) or human liver cells (hepatitis). Human beings and other organisms have

developed specialized defense mechanism to protect from viruses. Among these defenses, the immune system is highly effective which can disable and kill viruses.

In present study, *insilico* molecular docking studies of ligand indole against NS5B RNA dependent RNA polymerase HCV (PDB ID: 3CSO) [10] has been carried out using induced fit docking protocol of Schrödinger 2009[11]. Based on docking score, glide energy and key active site interactions, ligands showing better binding affinity compared to -crystalized ligand{(11S)-10-acetyl-11-[4-(benzyloxy)-3-chlorophenyl]-3,3-dimethyl-2,3,4,5,10,11-hexahydro-1H-dibenzo[b,e][1,4]diazepin- 1-one} were selected and the results were tabulated (Table 6).The pictures were generated using PyMol[12].In view of the medicinal importance of indole derivatives, in the present communication we have synthesized and the results are presented.

MATERIALS AND METHODS

SYNTHESIS

A mixture of (Z)-2-((2-formyl-3-methyl-1H-indol-1-yl)methyl)-3-phenylacrylonitrile (1 mmol) with *N*-methylhydroxylamine hydrochloride (1.1 mmol) and ethanol (5 ml) were placed in a round bottom flask and refluxed for 6 hrs. After completion of the reaction as indicated by TLC, the reaction mixture was concentrated under reduced pressure. The crude product was diluted with water and extracted with ethylacetate (20 ml). The organic layer washed with brine solution (10 ml) and concentrated. The crude product was purified by column chromatography (10% EtOAc and Hexanes) to provide the desired pure product as colourless solid with excellent yield.

Crystallographic Determinations

A colourless block single crystal with dimensions of 0.20 mm×0.20 mm×0.20 mm was selected for measurement. Diffraction data of the single crystal were collected by $\phi\sim\omega$ scan mode using a graphite-monochromatic Mo $K\alpha$ radiation ($\lambda = 0.71073 \text{ \AA}$) at 293 (2) K on a Bruker Smart Apex CCD diffractometer. The structure was solved by direct methods [13] using SHELXS-97 and the structure were refined by full-matrix least-squares techniques on F^2 using SHELXL-97. Non-hydrogen atoms were refined anisotropically, while hydrogen atoms were added according to theoretical models. A summary of the crystallographic data and refinement parameters is listed in Table 1. Selected bond length, bond angles and torsion angle for non-hydrogen atoms are listed in Tables 2, Tables 3 and Tables 4. The hydrogen bond interactions are listed in Table 5.

The bond lengths and bond angles of indole are good agreement with the values reported in related literature [14]. The indole moiety is planar, the fused benzene and pyrrole rings creates the dihedral angle of $0.91(5)^\circ$. Atoms C19 lie out of the least-squares plane of the indole ring by $0.060(2) \text{ \AA}$, respectively. The sum of the bond angles at nitrogen atoms of the indole ring is 360° in accordance with sp^2 hybridized state.

The five membered pyrrolidine (C6/C7/C9/C10/N1) ring adopts envelope conformation. The puckering parameters are $[15]q_2=0.347(2) \text{ \AA}$, $\Phi_2= 179.44(9)^\circ$. The other isoxalidine ring (N3/O1/C7-C9) adopts envelope conformation. The puckering parameters are $[15]q_2=0.254(2) \text{ \AA}$, $\Phi_2= -138.76(9)^\circ$. The endocyclic angles at C5 atom in the indole moiety is widened to $123.6(5)^\circ$ while those at C4 atom is contracted to $116.5(5)^\circ$. This would appear to be a direct effect caused by the fusion of the pyrrole with benzene ring. The bond length $C20-N2 = 1.141(6) \text{ \AA}$, and the bond angle $C7-C20-N2 = 177.5(5)^\circ$ reveal the triple bond character.

MOLECULAR MODELING STUDIES OF INDOLE COMPOUND WITH HCV NS5B POLYMERASE AS A TARGET PROTEIN

The HCV polymerase (NS5B) is a focus of HCV drug discovery efforts. The main functional role of NS5B in the virus life cycle is the assembly of the replicase complex at the endoplasmic reticulum membrane and the amplification of the genetic material through RNA-dependent RNA polymerase (RdRp) activity. Development of HCV NS5B polymerase inhibitors, particularly at allosteric binding sites, has gained increasing interests in recent years.

RESULTS AND DISCUSSION

In this study, we have used glide docking to study the binding orientations and predict binding affinities of indole compound. The results obtained from this study would be useful in both understanding the inhibitory mode of indole derivatives as well as in rapidly and accurately predicting the activities of newly designed inhibitors on the basis of docking scores. Since hydrogen bonds play a significant role in the structure and function of biological molecules, the ligand-receptor interactions were analyzed on the basis of H bonding. The docking score, glide energy and hydrogen bond interactions, are tabulated (Table 6). The molecule show better docking score -6.11 and

reasonable glide energy are -40.17 compared to cocrystallised inhibitor (-5.69 and -56.04). The carbonitrile group of indole interacts with the nitrogen atom of Arg 386 and Tyr 415 at a distance of 3.49 \AA and 2.86 \AA respectively as shown in Fig.7. The compound could be thought of possessing potent activity compared to the co-crystallized ligand (inhibitor) from our *in silico* docking studies. For better understanding of inhibition, molecular dynamics studies are needed so that the interactions with key active site residues and thermodynamic properties can be validated.

Table 1 Crystal data for INDOLE

Parameters	INDOLE
Empirical formula	C ₂₁ H ₁₉ N ₃ O
Formula weight	329.39
Wavelength(Å)	0.71073
Crystal system	Orthorhombic
Space group	Pca2 ₁
Unit cell dimensions	
a(Å)	16.288(4)
b(Å)	6.1798(5)
c(Å)	17.246(4)
α(°)	90
β(°)	90
γ(°)	90
Volume(Å ³)	1735.9(7)
Z, Calculated density(Mg/m ³)	4, 1.260
Absorption coefficient(mm ⁻¹)	0.079
F(000)	696
Crystal size(mm)	0.20 x 0.20 x 0.20
θrange (°)	2.50 to 27.82
Limiting indices	-20<=h<=20 -6<=k<=6 -19<=l<=20
Reflections collected / unique	8317 / 2841 [R(int) = 0.0806]
Refinement method	Full-matrix least-squares on F ²
Data / restraints / parameters	2841 / 1 / 228
Goodness-of-fit on F ²	0.974
Final R indices [I>2σ(I)]	R1 = 0.0596, wR2 = 0.1245
R indices (all data)	R1 = 0.1215, wR2 = 0.1494
Largest diff. peak and hole(eÅ ⁻³)	0.186 and -0.236

Table 2 Bond length (Å) involving the non-hydrogen atoms of INDOLE

Atoms	Length	Atoms	Length
C(1)-C(2)	1.370(7)	C(9)-C(10)	1.511(6)
C(1)-C(12)	1.400(6)	C(10)-C(11)	1.348(6)
C(2)-C(3)	1.393(6)	C(10)-N(1)	1.375(6)
C(3)-C(4)	1.384(7)	C(11)-C(12)	1.460(6)
C(4)-C(5)	1.382(6)	C(11)-C(19)	1.490(6)
C(5)-N(1)	1.386(6)	C(13)-C(14)	1.376(6)
C(5)-C(12)	1.412(5)	C(13)-C(18)	1.383(7)
C(6)-N(1)	1.454(6)	C(14)-C(15)	1.368(7)
C(6)-C(7)	1.543(6)	C(15)-C(16)	1.373(8)
C(7)-C(20)	1.476(7)	C(16)-C(17)	1.357(8)
C(7)-C(8)	1.554(6)	C(17)-C(18)	1.375(7)
C(7)-C(9)	1.556(6)	C(20)-N(2)	1.141(6)
C(8)-O(1)	1.416(5)	C(21)-N(3)	1.466(6)
C(8)-C(13)	1.509(6)	N(3)-O(1)	1.440(5)
C(9)-N(3)	1.457(5)		

Table 3 Bond angles (°) involving the non-hydrogen atoms of INDOLE

Atoms	Angle	Atoms	Angle
C(2)-C(1)-C(12)	118.9(5)	C(10)-C(11)-C(12)	105.1(4)
C(1)-C(2)-C(3)	121.8(5)	C(10)-C(11)-C(19)	129.4(4)
C(4)-C(3)-C(2)	121.3(5)	C(12)-C(11)-C(19)	125.5(4)
C(5)-C(4)-C(3)	116.5(5)	C(1)-C(12)-C(5)	117.9(5)
C(4)-C(5)-N(1)	130.4(4)	C(1)-C(12)-C(11)	133.9(4)
C(4)-C(5)-C(12)	123.6(5)	C(5)-C(12)-C(11)	108.2(4)
N(1)-C(5)-C(12)	106.0(4)	C(14)-C(13)-C(18)	118.9(5)
N(1)-C(6)-C(7)	101.2(3)	C(14)-C(13)-C(8)	120.0(5)
C(20)-C(7)-C(6)	110.6(3)	C(18)-C(13)-C(8)	121.1(4)
C(20)-C(7)-C(8)	112.2(3)	C(15)-C(14)-C(13)	120.2(5)
C(6)-C(7)-C(8)	113.1(4)	C(14)-C(15)-C(16)	121.3(6)
C(20)-C(7)-C(9)	114.4(4)	C(17)-C(16)-C(15)	118.2(6)
C(6)-C(7)-C(9)	106.9(3)	C(16)-C(17)-C(18)	121.9(6)
C(8)-C(7)-C(9)	99.1(3)	C(17)-C(18)-C(13)	119.5(5)
O(1)-C(8)-C(13)	109.7(4)	N(2)-C(20)-C(7)	177.5(5)
O(1)-C(8)-C(7)	105.9(3)	C(10)-N(1)-C(5)	109.3(3)
C(13)-C(8)-C(7)	118.1(4)	C(10)-N(1)-C(6)	114.9(3)
N(3)-C(9)-C(10)	114.8(3)	C(5)-N(1)-C(6)	135.8(4)
N(3)-C(9)-C(7)	107.8(3)	O(1)-N(3)-C(9)	106.2(3)
C(10)-C(9)-C(7)	101.2(3)	O(1)-N(3)-C(21)	104.7(4)
C(11)-C(10)-N(1)	111.4(3)	C(9)-N(3)-C(21)	111.8(3)
C(11)-C(10)-C(9)	139.1(4)	C(8)-O(1)-N(3)	111.5(3)
N(1)-C(10)-C(9)	109.3(4)		

Table 4 Torsion angles (°) involving the non-hydrogen atoms of INDOLE

Atoms	Angle	Atoms	Angle
C(1)-C(2)-C(3)-C(4)	-1.7(9)	C(9)-C(10)-C(11)-C(12)	-175.5(4)
C(2)-C(3)-C(4)-C(5)	1.0(8)	C(21)-N(3)-C(9)-C(10)	151.1(4)
C(2)-C(1)-C(12)-C(5)	0.7(7)	C(10)-C(9)-N(3)-O(1)	-95.3(4)
C(2)-C(1)-C(12)-C(11)	-179.5(5)	C(10)-C(11)-C(12)-C(1)	-178.5(5)
C(3)-C(4)-C(5)-N(1)	-180.0(5)	C(10)-C(11)-C(12)-C(5)	1.3(5)
C(3)-C(4)-C(5)-C(12)	0.5(7)	C(11)-C(10)-N(1)-C(6)	-178.2(4)
C(4)-C(5)-N(1)-C(6)	-0.7(8)	C(11)-C(10)-N(1)-C(5)	0.9(4)
C(4)-C(5)-C(12)-C(11)	178.8(4)	C(12)-C(1)-C(2)-C(3)	0.8(8)
C(4)-C(5)-C(12)-C(1)	-1.3(7)	C(12)-C(5)-N(1)-C(10)	0.0(5)
C(4)-C(5)-N(1)-C(10)	-179.6(5)	C(12)-C(5)-N(1)-C(6)	178.8(5)
C(6)-C(7)-C(9)-N(3)	-145.7(3)	C(13)-C(14)-C(15)-C(16)	-1.1(9)
C(6)-C(7)-C(8)-O(1)	142.5(4)	C(13)-C(8)-O(1)-N(3)	-150.7(3)
C(6)-C(7)-C(8)-C(13)	-94.2(5)	C(14)-C(13)-C(18)-C(17)	-1.0(7)
C(6)-C(7)-C(9)-C(10)	-24.9(4)	C(14)-C(15)-C(16)-C(17)	0.0(9)
C(6)-C(7)-C(20)-N(2)	-2(11)	C(15)-C(16)-C(17)-C(18)	0.6(9)
C(7)-C(8)-C(13)-C(14)	98.4(5)	C(16)-C(17)-C(18)-C(13)	0.0(9)
C(7)-C(8)-C(13)-C(18)	-80.0(5)	C(18)-C(13)-C(14)-C(15)	1.6(7)
C(7)-C(9)-N(3)-C(21)	-97.0(4)	C(19)-C(11)-C(12)-C(5)	-178.5(4)
C(7)-C(8)-O(1)-N(3)	-22.3(5)	C(19)-C(11)-C(12)-C(1)	1.7(8)
C(7)-C(6)-N(1)-C(10)	-13.6(5)	C(20)-C(7)-C(8)-O(1)	-91.5(4)
C(7)-C(6)-N(1)-C(5)	167.6(5)	C(20)-C(7)-C(8)-C(13)	31.7(6)
C(7)-C(9)-N(3)-O(1)	16.6(4)	C(20)-C(7)-C(9)-N(3)	91.6(4)
C(7)-C(9)-C(10)-C(11)	-168.9(5)	C(20)-C(7)-C(9)-C(10)	-147.6(3)
C(7)-C(9)-C(10)-N(1)	16.9(4)	C(21)-N(3)-O(1)-C(8)	122.1(4)
C(8)-C(7)-C(9)-N(3)	-28.1(4)	N(1)-C(6)-C(7)-C(20)	148.7(4)
C(8)-C(7)-C(9)-C(10)	92.8(3)	N(1)-C(6)-C(7)-C(8)	-84.5(4)
C(8)-C(13)-C(14)-C(15)	-176.9(5)	N(1)-C(6)-C(7)-C(9)	23.6(4)
C(8)-C(7)-C(20)-N(2)	-129(11)	N(1)-C(5)-C(12)-C(11)	-0.8(5)
C(8)-C(13)-C(18)-C(17)	177.4(5)	N(1)-C(10)-C(11)-C(12)	-1.3(4)
C(9)-C(10)-N(1)-C(6)	-2.3(5)	N(1)-C(5)-C(12)-C(1)	179.0(4)
C(9)-N(3)-O(1)-C(8)	3.7(4)	C(19)-C(11)-C(10)-N(1)	178.5(5)
C(9)-C(7)-C(20)-N(2)	119(11)	N(3)-C(9)-C(10)-C(11)	-53.1(7)
C(9)-C(10)-N(1)-C(5)	176.8(3)	N(3)-C(9)-C(10)-N(1)	132.6(3)
C(9)-C(10)-C(11)-C(19)	4.3(9)	O(1)-C(8)-C(13)-C(18)	41.3(6)
C(9)-C(7)-C(8)-O(1)	29.7(4)	O(1)-C(8)-C(13)-C(14)	-140.3(4)
C(9)-C(7)-C(8)-C(13)	153.0(4)		

Table 5 Hydrogen bond interactions for INDOLE [Å and °]

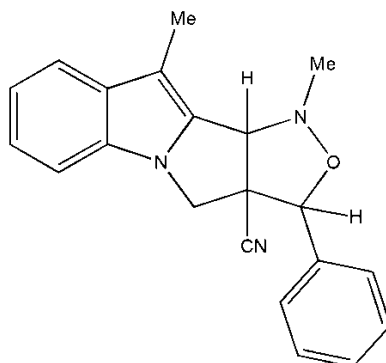
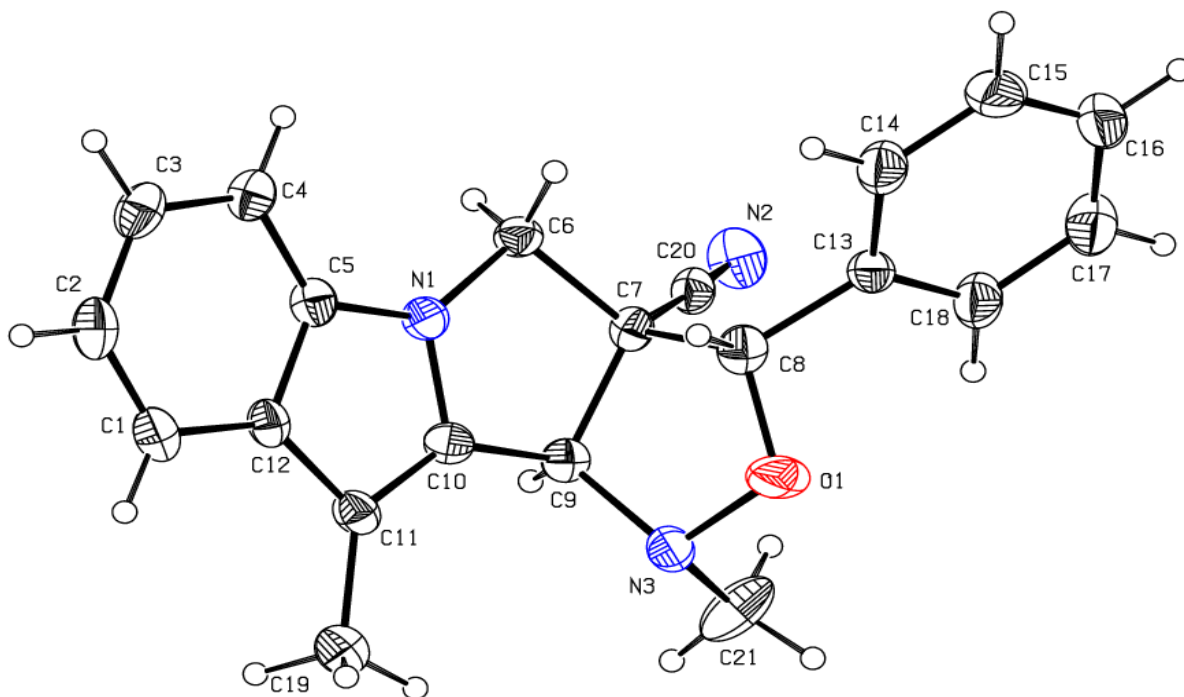
Compounds	D-H...A	D-H	H...A	D...A	D-H...A
INDLOE	C6-H6A...N2 ⁱ	0.97	2.58	3.440(7)	149
	C9-H9...Cg(4) [#]	0.98	2.46	3.397(4)	160

Symmetry Codes

- (i) $x, y-1, z$
(ii) $x, y+1, z$

Table 6 Docking results of INDOLE with RdRp-NS5B along with intermolecular hydrogen bond interactions with active site residues

Compound Category		Docking score	Glide evdw	Glide ecoul	Glide energy	Intermolecular H-Bonding	Distance (Å)
Co-Crystal-ligand (PDB ID: 3CSO)	S.NO	-5.69	-50.59	-5.53	-56.04	TYR 448 N-H...O	3.07
Indole	I	-6.11	-34.34	-5.82	-40.17	ARG386 N-H...N	3.49
						TYR 415 O-H...N	2.86

DIAGRAM**Fig.1.** Chemical Diagram for INDOLE**Fig.2.** Perspective view of the INDOLE with the atom numbering scheme Displacement ellipsoids is drawn at 30% probability level

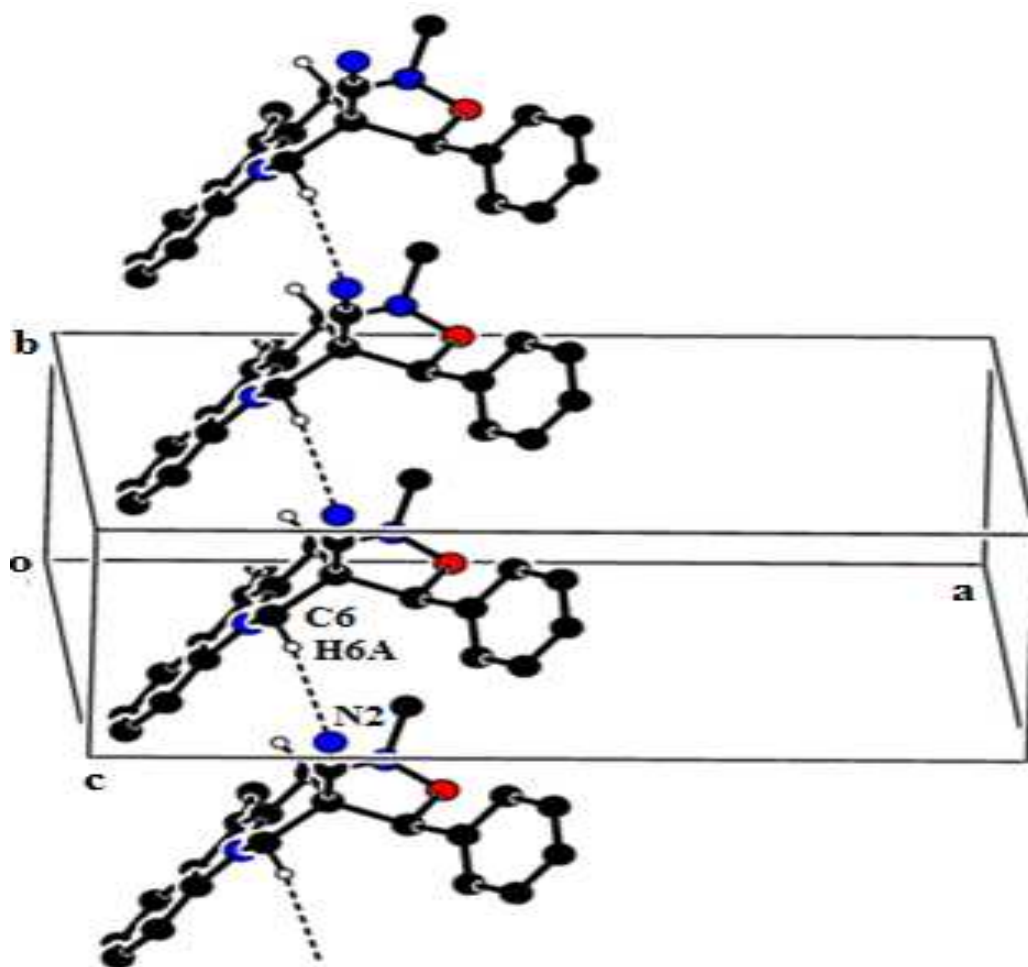


Fig.3. Packing of the molecules viewed down the *c*-axis for INDOLE



Fig.4. Cartoon representation of NS5B RNA polymerase with Co-crystal(PDB ID: 3CSO)

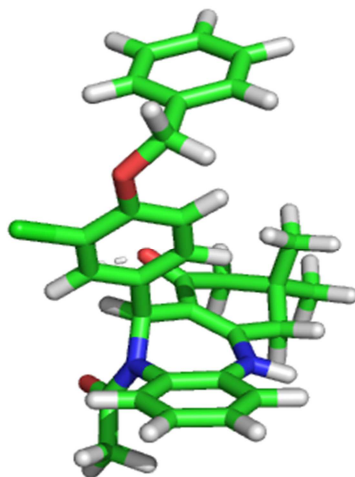


Fig.5. PyMol representation of co-crystal ligand

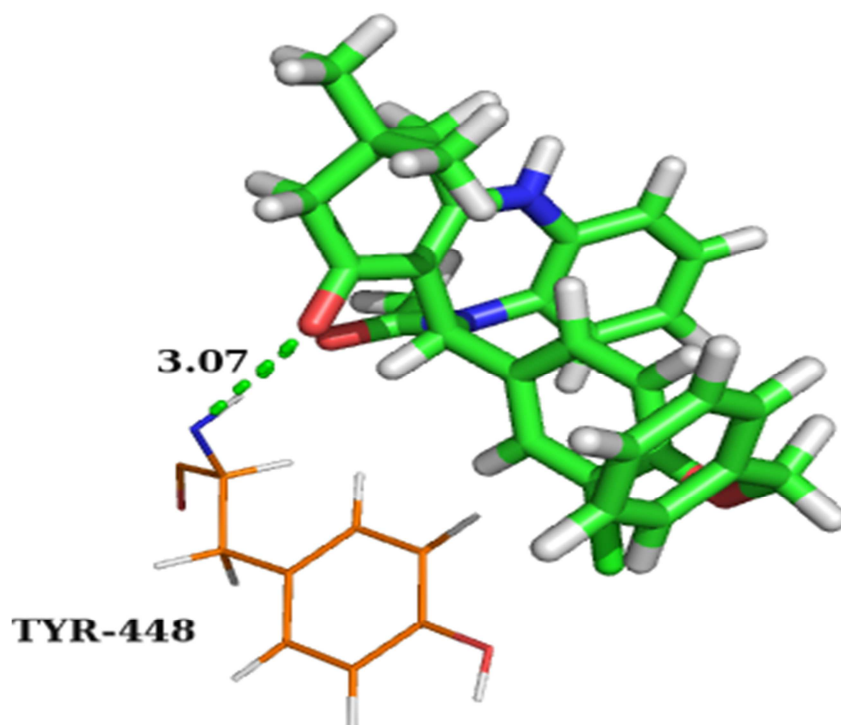


Fig.6 Interactions exhibited by co-crystallized ligand with the active site residues of 3CSO

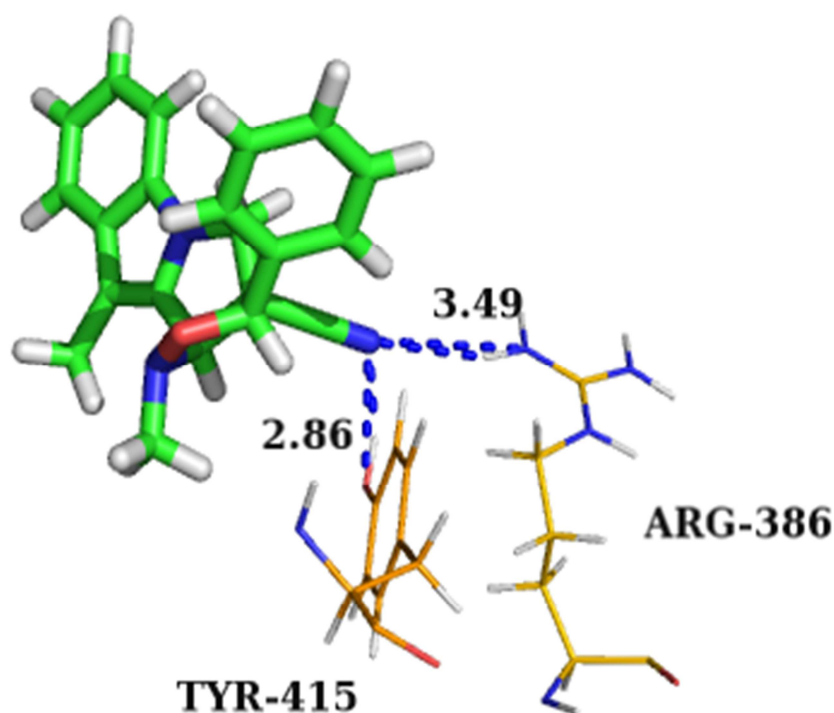


Fig.7 Interactions exhibited by INDOLE ligand with the active site residues of 3CSO

Packing Features

The packing of the molecules of indole is viewed down c-axis shown in Fig.3; it is through weak C-H...N, and C-H... π intermolecular interactions (Table 5) in addition to van der Waals forces. The molecules at (x, y, z and x, y-1, z) are linked by C6-H6A...N2 hydrogen bond. The packing was further stabilized by C9-H9...Cg(4) interaction.

Acknowledgements

VS thanks Dr Babu Varghese, Senior Scientific Officer, SAIF, IIT, Chennai, India, for the X-ray intensity data collection and Prof. D. Velmurugan, Head of the Department, CAS in Crystallography & Biophysics, University of Madras, for using the software to carry out my docking studies.

Computational detail

Data collection: SMART [16]; cell refinement: SAINT [16]; data reduction: SAINT; program(s) used to solve structure: SHELXS97 [13]; program(s) used to refine structure: SHELXL97 [13] molecular graphics: PLATON [17]; software used to prepare material for publication: SHELXL97 and PARST [18].

REFERENCES

- [1] J. Quetin-Leclercq *J. Pharm. Belg.*, **49**, 181-192. (1994). (Farhanullah et al., 2004).
- [2] J. Rodriguez F, Temprano, C. Esteban-Calderon, M. Martinez-Ripoll, S. Garcia-Blanco, *Tetrahedron*. **41**, 3813-3823 (1985).
- [3] N. Okabe and Y. Adachi, (1998). *Acta Cryst.* **C54**, 386-387.
- [4] D. Schollmeyer, G. Fischer and U. Pindur, (1995). *Acta Cryst.* **C51**, 2572-2575.
- [5] A. Andreani, M. Granaiola, A. Leoni, A. Locatelli, R. Morigi, M. Rambaldi, G. Giorgi, L. Salvini, and V. Garaliene, (2001). *Anticancer Drug Des.* **16**, 167-174.
- [6] H. X. Wang, T. B. Ng, *Comput. Biochem. Physiol. C. Toxicol. Pharmacol.* **132**, 261-268 (2002).
- [7] A. L. Spek, (2009). *Acta Cryst.* **D65**, 148-155.
- [8] A. Tsotinis, A. Varvaresou, T. Calogeropoulou, T. Siatra-Papastakoudi, A. Tiligada, *Arzneim.-Forsch.* **47**, 307-310 (1997).
- [9] J. Quetin-Leclercq, A. Favel, G. Balansard, P. Regli, P. Angenot, *Planta Med.*, **61**, 475-477 (1995).
- [10] O. Nyanguile, F. Pauwels, W. V. D Broeck, C.W. Boutton, L. Quirynen, T. Ivens, L.V.D. Helm, G. Vandercruyssen, W. Mostmans, F. Delouvroy, P. Dehertogh, M.D. Cummings, J.F. Bonfanti, K.A. Simmen, P. Raboisson, *Antimicrobial Agents and Chemotherapy*. Vol. **52**, No. 12 p. 4420-4431 (2008).
- [11] Schrödinger Suite 2009, LLC, New York, NY, 2009.

- [12] W. L. DeLano, (2002). The PyMOL Molecular Graphics System. DeLano Scientific, San Carlos, CA, USA. <http://www.pymol.org>.
- [13] G. M. Sheldrick, *Acta Cryst.* **A64**, 112–122. (2008).
- [14] G. Jagadeesan, K. Sethusankar, R. Prasanna, R. Raghunathan, *Acta Cryst.* **E68**, o2505–o2506 (2012).
- [15] D. Cremer J. A. Pople, (1975). *J. Am. Chem. Soc.* **97**, 1354–1358 (1975).
- [16] Bruker APEX2, SAINT, XPREP and SADABS. Bruker AXS Inc., Madison, Wisconsin, USA. (2004).
- [17] A. L. Spek, (2009). *Acta Cryst.* **D65**, 148–155.
- [18] M. Nardelli, *Acta Cryst.* **C39**, 1141–1142 (1983).